Tuning of Particle Size, Surface Morphology and Optical Band Gap of Tricobalt Tetraoxide (Co$_3$O$_4$) Nanostructures via Solvent Dependent Assembly

Gajendiran J[1*], Parthasaradhi Reddy C[1], Senthil VP[1], Gokul Raj S[2]

[1]*Department of Physics, Veltech Dr. RR & Dr. SR University, Avadi-600062, Chennai, India*
[2]*Department of Physics, C. Kandaswami Naidu College for Men, Chennai-600102, India*

ABSTRACT

The particle size and optical band gap of Co$_3$O$_4$ nanostructures is varied simply by varying the solvent (hypodicabonous acid, cologne spirit and hydric acid) of precursor containing cobalt acetate dehydrate and white caustic pellets. In addition, the detailed mechanism for the surface morphology formation of the Co$_3$O$_4$ nanostructures has been discussed.

Keywords: Surface Morphology, Nanostructures, FTIR, SEM, Optical Band gap

INTRODUCTION

Past few years, different kinds of transition tri metal tetra oxides (TTMTO) nanostructures, such as hausmanite, magnetite and tri cobalt tetra oxide have attracted much attention due to their interesting physico-chemical properties and thus, have been widely used for optoelectronic devices, lithium-ion battery, gas sensors and as catalysts [1-3]. Among the tri metal tetra oxides, tri cobalt tetra oxide (Co$_3$O$_4$) nanostructures have attracted increasing interest for both fundamental and practical reasons due to the stable phase, controlled oxidation state, and dual optical band gap etc. It is an p-type semiconductor, which makes it suitable for dye-sensitized solar cells [4], gas sensors [5], Li-ion batteries [6,7], optoelectronic [8,9] and magnetic storage devices [10]. The valuable functions greatly depend on the morphology and particle size of Co$_3$O$_4$ nanostructures [11,12].

Various physico-chemical routes have been developed to prepare the Co$_3$O$_4$ nanostructures, namely, thermal decomposition method [13], polyol [14], microwave reflux [15], chemical vapor deposition (CVD) [15], electro deposition followed ozene treatment [16], chemical combustion [17], and hydro or alcoholthermal method, etc [18]. However, most of the methods have one or more drawbacks, such as the use of expensive equipment, use of inert gas atmosphere, complicated synthetic steps, prolonged reaction times, and high synthetic temperatures. Therefore, the development of simple, inexpensive, short time synthesis and nontoxic methods for the preparation Co$_3$O$_4$ nanostructures at relatively low temperature is still demanded. Among the synthesis routes, hydro or alcothermal synthesis of Co$_3$O$_4$ have been research hotspots due to the advantage of less agglomeration with good crystallinity to enhance optical activities, and outstanding performance of nanosized electronic and optical devices. The various of cobalt salt, precipitating agent, surfactant, solvent (water, water-ethylene glycol and water-butanol), pH value of the suspension and the amount of oxidant H$_2$O$_2$ on the morphology and structure of Co$_3$O$_4$ have been investigated by Yang et al. [18]. Tuning of super capacitors properties of Co$_3$O$_4$ nanostructures by varying the solvent have been investigated by Yang et al. [19].
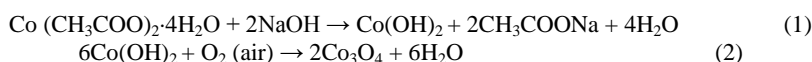
In this paper, the comparative studies of the structural, spectral, morphological and optical property of the Co$_3$O$_4$ nanostructures in the presence of three different solvents (Hypodicabonous acid, cologne spirit and hydric acid) containing cobalt acetate dehydrate and white caustic pellets, by the hydro or alcohol thermal method.

MATERIALS AND METHODS

0.1 M of cobalt acetate dehydrate (Co(CH$_3$COO)$_2$.2H$_2$O) and 0.2 M of white caustic pellets (NaOH) was separately dissolved in 40 mL of three different solvents such as hypodicabonous acid (HO-CH$_2$-CH$_2$-OH), cologne spirit (C$_2$H$_5$-OH) and hydric acid (H$_2$O). The NaOH solution was slowly added drop wise to the cobalt acetate solution under electromagnetic stirring for 1 h. After that, the translucent solution was sealed in stainless steel autoclave maintains at 180°C for 12 h at a ramping rate of 5°C/min. The obtained precipitate was washed several times with ethanol due to the decreased the agglomeration by preventing the formation of Co$_3$O$_4$ particles. Then, the black colored Co$_3$O$_4$ nanopowder obtained were calcined at 450°C for 2 h at a ramping rate of 5°C/min.

In present experiment, after mixing the two translucent solutions containing Co(CH$_3$COO)$_2$·4H$_2$O and NaOH, the precursor Co(OH)$_2$ nuclei were

formed by the reaction of Co^{2+} cations with OH^- anions [20]. As a consequence, the transferred to the autoclave and subsequent calcination lead to the formation of Co_3O_4 nanopowder. The formation of Co_3O_4 nanopowder can be expressed as follows:

$$Co\ (CH_3COO)_2 \cdot 4H_2O + 2NaOH \rightarrow Co(OH)_2 + 2CH_3COONa + 4H_2O \qquad (1)$$
$$6Co(OH)_2 + O_2\ (air) \rightarrow 2Co_3O_4 + 6H_2O \qquad (2)$$

The prepared Co_3O_4 samples, characterized by the powder XRD pattern, were collected on a Schimadzu model XRD 6000 with CuK_α radiation (λ=1.5417Å). The functional groups were identified by the FTIR spectra (Nicolet 305 spectrometer). The morphological studies were carried out by the SEM (JEOL-JEM-3010) and Transmission Electron Microscope (TEM) (Philips model CM 20) analyses. The optical properties were studied by the UV-visible absorption spectra (Varian cary5E spectrophotometer).
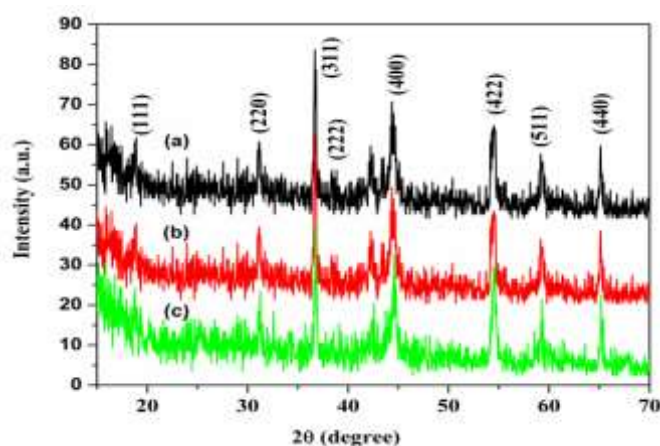
RESULTS AND DISCUSSION

Figure 1: XRD patterns of (a) Hypodicabonous acid, (b) Cologne spirit and (c) Hydric acid assisted Co₃O₄ powders

The phase purity, crystal structure, and average crystallite size of the Co_3O_4 prepared, was determined by the powder X-ray diffraction (XRD) analysis. Figure 1 displays the XRD pattern of hypodicabonous acid, cologne spirit and hydric acid assisted Co_3O_4 nanopowder obtained by solution method. The peaks are appearing due to the reflection from the (111), (220), (311), (222), (400), (422), (511) and (440) planes of the cubic spinel structure of Co_3O_4. The XRD pattern of the synthesized Co_3O_4 samples is well matched with the standard cubic structure of Co_3O_4 (JCPDS No.43-1003) [14]. No characteristic peaks of impurity phases are present, indicating the high purity of the Co_3O_4 samples. The average crystallite size is calculated by using Debye Scherer's formula; only if the prepared samples were spherical, they were applicable. If broad peaks were observed in the XRD pattern, it indicates that the Full Width Half Maximum (FWHM) value is high, resulting in the average particle size of the prepared sample being smaller. If sharp peaks were observed in the XRD pattern, it means, that the prepared samples were of a well crystalline nature, and also, that the full width half maximum value is smaller; this reflects that the average crystallite size being larger. The slightly broad peaks of the hypodicabonous acid and cologne spirit assisted Co_3O_4 samples were observed from the XRD pattern compared than the hydric acid assisted sample due to the smaller crystallite size. Further, the average crystallite size of the Co_3O_4 samples are calculated, by using the Debye Scherer's formula such as ~30, 40 and 45 nm for hypodicabonous acid, cologne spirit and hydric acid, respectively. Moreover, the diffraction peaks indicated the polycrystalline nature, which is later proved by the Selected Area (Electron) Diffraction (SAED) pattern.

The functional groups information of the synthesized products was further obtained by the FTIR studies, which was essential in the range of 400-4000 cm^{-1}. Figure 2 compares the FTIR spectra for hypodicabonous acid, cologne spirit and hydric acid assisted samples, in which a similar profile can be observed for all curves. They show that the peaks located at ~1626 and 3440 cm^{-1} correspond to the bending modes of H_2O and stretching vibration of the OH groups, respectively. The strong two absorption peaks at ~ 586 and 666 cm^{-1} confirm the formation of the Co-O bond [20]. In general, the peaks at ~586 cm^{-1} is assigned to the stretching vibration of Co^{3+}-O bond, where Co^{3+} is an octahedral position and the another peaks at ~666 cm^{-1} is the stretching vibration of Co^{2+}-O bond, where Co^{2+} is an tetrahedral position, respectively [11]. Based on the above FTIR studies, the prepared sample confirms the formation of cobalt oxide, which is also support to the XRD studies.
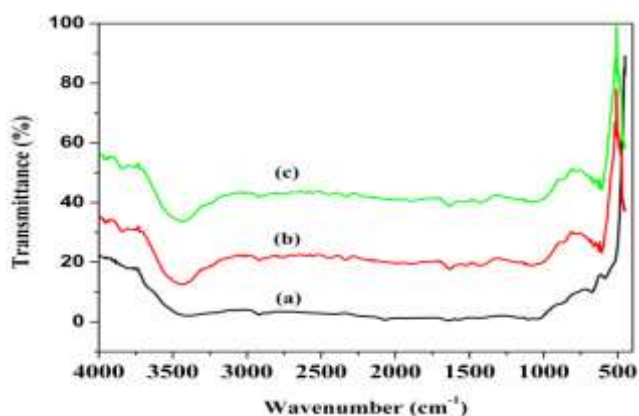

Figure 2: FTIR spectra of (a) Hypodicabonous acid, (b) Cologne spirit and (c) Hydric acid assisted Co₃O₄ powders
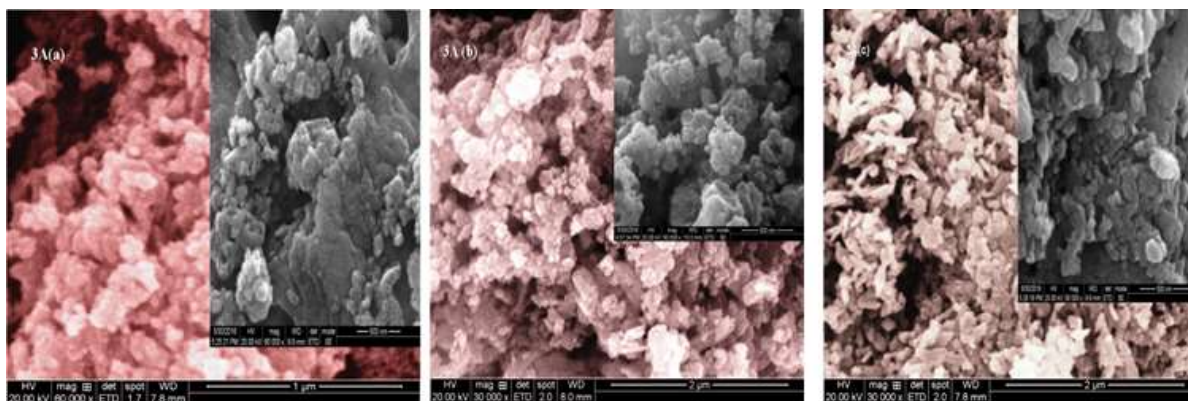
Figure 3A: SEM images of (a) Hypodicabonous acid, (b) Cologne spirit and (c) Hydric acid assisted Co₃O₄ nanostructures

Surface morphology, particle dispersed nature and average particle sizes of the prepared Co3O4 powder were investigated by the SEM studies (Figure 3A). It can be seen that the uniform nanocrystallite Co₃O₄ particles had sphere shapes with weak agglomeration using hypodicabonous acid solvent (Figure 3A (a) and its average particles size is about ~ 30 nm (High magnification image as shown in insert of Figure 3A (a). Using cologne spirit solvent (Figure 3A (b), cobalt oxide particles exhibited semi sphere with minor particle agglomeration and its average particle size ~ 40 nm (high magnification image as shown in insert of Figure 3A (b). Using hydric acid solvent (Figure 3A (c), Co₃O₄ particles shows elongated spherical shaped and its average particle size ~ 45 nm (High magnification image as shown in insert of Figure 3A (c).

In addition, hypodicabonous acid assisted Co₃O₄ sample were further characterized by the TEM, and shown in Figure 3B. Looking at carefully observed from the microstructure study, which seems to be formed by the dispersed of several spherical shaped particles with the average particle size of Co₃O₄ nanoparticles ~30 nm.
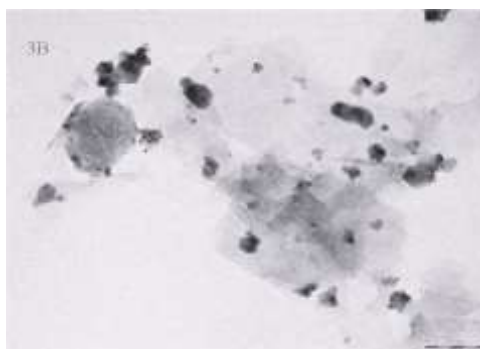

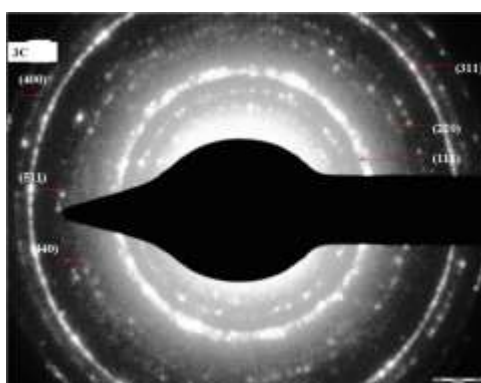**Figure 3B: TEM image of hypodicabonous acid assisted Co₃O₄ nanoparticles**

Figure 3C: SAED pattern of the hypodicabonous acid assisted Co₃O₄ nanoparticles

Moreover, several diffraction rings in the SAED pattern of the hypodicabonous acid assisted Co₃O₄ nanoparticles are shown in Figure 3C. The diffraction patterns exhibit the lattice planes (111), (220), (311), (400), (511) and (440) of the poly crystalline nature of the cubic spinel structure of the Co₃O₄ particles (JCPDS No.43-1003) [14], which is in good agreement with the XRD result. A schematic formation of Co₃O₄ nanoparticles is shown in Figure 3D.
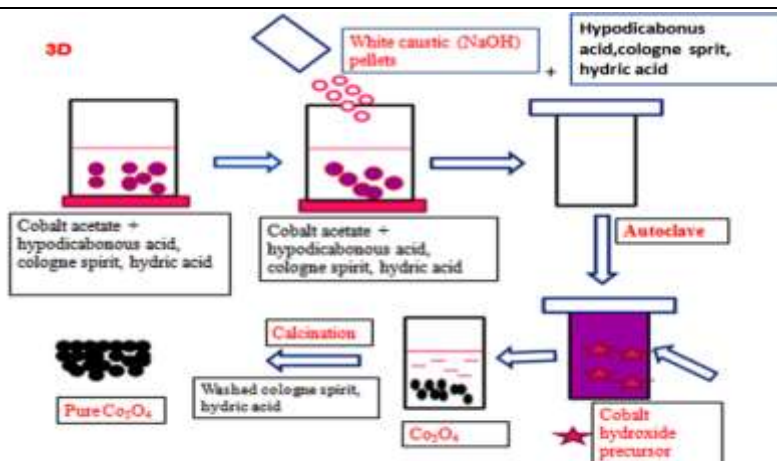
Figure 3D: Schematic formation of Co$_3$O$_4$ nanostructures

Slightly dispersed spherical, aggregated spherical and elongated spherical like nanostructures of the Co$_3$O$_4$ samples obtained from the hypodicabonous acid, cologne spirit and hydric acid solvents can be affected by considering some physical and chemical properties of solvents, whose formation mechanisms are proposed based on the above observation. The hypodicabonous acid, cologne spirit and hydric acid solvents used in systems will change the systems' viscosity and surface tensions, which will in turn, affect the kinetics of the crystal growth [18,19,21-24]. The viscosity of solvents has a major impact on the nucleation and growth of crystal. In the alcoholic solvents (hypodicabonous acid and cologne spirit) assisted samples, after the crystallite nuclei are generated, the slow diffusion rate of ions, due to the high viscosity of the solvent, greatly suppresses the intrinsic anisotropic growth, resulting from the dispersed spherical shaped Co$_3$O$_4$ due to the alcoholic solvents with high viscosity and low surface tension compared than the hydric acid solvent [18,19,21-23]. The crystals are more likely to grow along the two dimensions; therefore, slightly dispersed and agglomerated Co$_3$O$_4$ spherical were formed in the hypodicabonous acid and cologne spirit assisted samples. In the case of hydric acid solvent with low viscosity and higher surface tension, the concentration of ions is relatively high, corresponding to a high super saturation and better ion diffusion capability. The tiny crystalline nuclei are generated in a highly supersaturated solution, followed by crystal anisotropic growth via ion-ion addition. The largely agglomerated spherical shaped Co$_3$O$_4$ particles were formed in the hydric acid assisted sample because the surface tension of water is higher than that of alcoholic solvents, the presence of hydric acid favors to increase the surface energy of Co$_3$O$_4$ particles so that the particles tend to aggregates.

The optical properties of nano-crystalline tri cobalt tetra oxides have been studied extensively in fast few years for translating their enhanced properties into practical applications [24-26]. As the size of the material becomes smaller, the optical band gap becomes larger thereby changing the optical properties of the material and making the material suitable for new applications and devices. The optical parameters such as optical absorption, optical band gap energy and nanosized effect of the prepared Co$_3$O$_4$ samples were detected by the UV-visible absorption spectroscopy. Figure 4A(a-c) shows the UV-visible absorption spectra of the Co$_3$O$_4$ samples, which can be assigned to the direct transition of electrons due to the presence of multiple absorption edges. It exhibits two absorptions peaks, which are assigned to the ligand-metal charge transfers (LMCT) $O^{II} \rightarrow Co^{II}$ and $O^{II} \rightarrow Co^{III}$, respectively, which is in good agreement with the previous literatures [24-26].
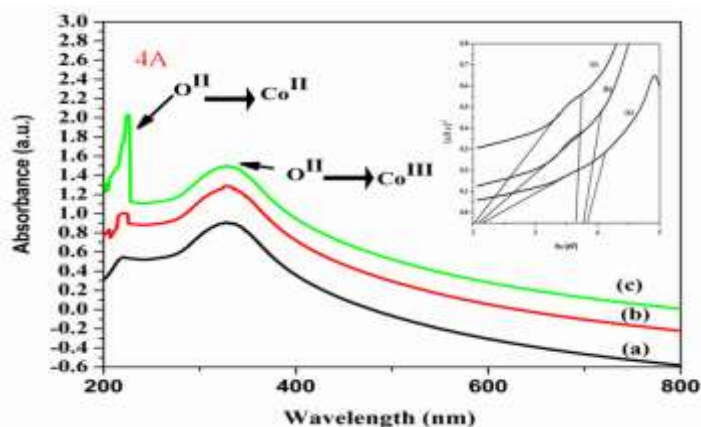

Figure 4A: UV-visible absorption spectra of (a) Hypodicabonous acid, (b) Cologne spirit and (c) Hydric acid assisted Co$_3$O$_4$ nanoparticles

The optical band gap energy (E$_g$) of the Co$_3$O$_4$ is given by the equation as:

$$\alpha h\nu = K(h\nu - E_g)^n \quad (3)$$

Where, hν is the photo energy, α is the absorption coefficient, K is a constant relative to the material, and n is either 1/2 for a direct transition or 2 for an indirect transition. The extrapolation curve of $(\alpha h\nu)^2$ versus hν is shown in the inset of Figure 4.

Generally, the exact values of band gap energy of the samples are estimated from the plots of $(\alpha h\nu)^2$ versus photon energy (hν) shown in Figure 4A. It involves a standard method of extrapolating the vertical and linear part of the curve to cut the energy axis. The value of energy at the point where the extrapolated line cuts x-axis is taken as band gap energy. The optical band gap of the as-obtained Co$_3$O$_4$ samples is calculated to be

2.15-3.85, 2.10-3.81 and 2.05-3.72 eV for hypodicabonous acid, cologne spirit and hydric acid respectively from the extrapolation curve, which were larger than the reported values for bulk Co_3O_4 (1.6 eV) [25]. The calculated optical band gap energy is higher than the bulk Co_3O_4, due to the absorption wavelength shift towards to the shorter wavelength. These phenomena ascribed to the blue shift, which is attributed to the nanosized effect and it can be used for optoelectronic devices [24-26]. Two optical band gaps for all Co_3O_4 samples suggesting direct allowed transitions, which can be understood in view of the Co_3O_4 band structure of Figure 4B. The valance band (VB) has a strong O 2p character, while the main contribution to the conduction band (CB) is given by the Co (II) 3d orbitals. The presence of Co (III) centers in Co_3O_4 gives rise to a sub band located inside the energy gap. Hence, E_{op1} correspond to the onset of O (-II) → Co(III) excitations, while E_{opt2} is the "true" energy gap corresponding to inter-bands transitions (IBT) (basic optical band gap energy, or valence to conduction band excitation).
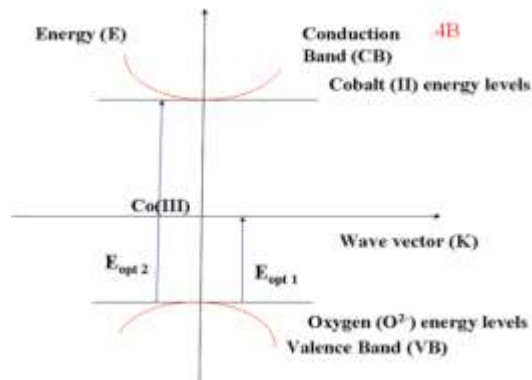

Figure 4B: Schematic representations of the band structure of Co_3O_4

CONCLUSION

In summary, we have successfully synthesized Co_3O_4 nanostructures via facile solution method by using the three different solvents. The synthesized nanostructures were investigated by various analytical methods including XRD, FTIR, SEM, TEM and UV-Visible studies. The XRD show the well-defined diffraction peaks with mono crystalline phase (cubic spinel structure) of Co_3O_4. The FTIR show the spectral absorption two different peaks at ~ 586 and 666 cm^{-1} corresponds to Co-O bonding, which confirms the prepared samples are formation of cobalt oxide. All the results demonstrate that the solvents have strong influence of particle size, surface morphology and optical band gap performance. Our investigation indicates that the hypodicabonous acid assisted Co_3O_4 nanoparticles are the better, in terms of the particle size and optical properties than the other cologne spirit and hydric acid solvents.

REFERENCES

[1] R. Son, S. Feng, H. Wang, C.M. Hou, *J. Solid. State. Chem.*, **2013**, 202, 57.

[2] T.K.O. Vuong, D.L. Tran, T.L. Le, D.V. Pham, H.N. Pham, T.H.L. Ngo, H.M. Do, X.P. Nguyen, *Mater. Chem. Phy.*, **2015**, 163, 537.

[3] M. Ghiasi, A. Malekzadeh, H. Mardani, *Mater. Sci. Semicond. Process.*, **2016**, 42, 311.

[4] J.K. Sharma, P. Srivastava, G. Singh, M.S. Akhtar, S. Ameen, *Mater. Sci. Eng. B.*, **2015**, 193, 181.

[5] J. Deng, R. Zhang, L. Wang, Z. Lou, T. Zhang, *Sensors and Actuators B.*, **2015**, 209, 449.

[6] G. Tong, Y. Liu, J. Guan, *J. Alloys. Comp.*, **2014**, 601, 167.

[7] S. Barkaoui, M. Haddaoui, H. Dhaouadi, N. Raouafi, F. Touati, *J. Solid State Chem.*, **2015**, 228, 226-231.

[8] A.F. Lima, *J. Phy. Chem. Solids.*, **2014**, 75, 148.

[9] S.A. Makhlouf, Z.H. Bakr, K.I. Aly, M.S. Moustafa, *Superlattic Microstrut.*, **2013**, 64, 107.

[10] G. Anandha Babu, G. Ravi, Y. Hayakawa, M. Kumaresavanji, *J. Magn. Magn. Mater.*, **2015**, 375, 184.

[11] Y. Teng, S. Yamamoto, Y. Kusano, M. Azuma, Y. Shimakaw, *Mater. Lett.*, **2010**, 64, 239.

[12] Y. Dong, K. He, L. Yin, A. Zhang, *Nanotechnology.*, **2007**, 18, 43.

[13] J. Jiang, L. Li, *Mater. Lett.*, **2007**, 61, 4894.

[14] Y. Ding, L. Xu, C. Chen, S. L.Suib, *J. Phys. Chem C.*, **2008**, 112(22), 8177.

[15] J. Zheng, B. Zhang, *Ceramics Inter.*, **2014**, 40, 11377.

[16] C.W. Kung, H.W. Chen, C.Y. Lin, R. Vittal, K.C. Ho, *J. Power Sources.*, **2012**, 214, 91.

[17] M.C.G. Merino, M.E.F. Derapp, M. Pinto, M.E. Etchechaoury, M.S. Lassa, J.M.M. Martinez, G.E. Lascalea, P.G. Vazquez, *Procedia Mater. Sci.*, **2015**, 9, 230.

[18] Y.P. Yang, K.L. Huang, R.S. Liu, *Trans. Nonferrous Met. Soc. China.*, **2007**, 17, 1082.

[19] W. Yang, Z. Gao, J. Ma, B. Wang, L. Liu, *Electrochemica Acta.*, **2013**, 112, 378.

[20] J. Gajendiran, V. Rajendran, *Mater. Sci. Semicond. Process.*, **2014**, 17, 59.

[21] Y. Liu, F. Yang, X. Yang, *Colloids. Surf. Eng. Aspects.*, **2008**, 312, 219.

[22] G.Q. Yuan, H.F. Jiang, C. Lin, S.J. Liao, *J. Cryst. Growth.*, **2007**, 303, 400.

[23] K.L. Foon, M. Kashif, U. Hashim, W.W. Liu, *Ceramics Inter.*, **2014**, 40, 753.

[24] Y. Chen, Y. Zhang, S. Fu, *Mater. Lett.*, **2007**, 61, 701-705.

[25] S. Vijayakumar, A. Kiruthika Ponnalagi, S. Nagamuthu, G. Muralidharan, *Electrochimica Acta.*, **2013**, 106, 500.

[26] L.H. Ai, J. Jiang, *Powder Tech.*, **2009**, 195, 11.